applied sciences

MDPI

Article

Dispersion Mechanism and Mechanical Properties of SiC Reinforcement in Aluminum Matrix Composite through Stir- and Die-Casting Processes

Sangmin Shin [1], Hyeonjae Park [1], Byeongjin Park [1], Sang-Bok Lee [1], Sang-Kwan Lee [1], Yangdo Kim [2], Seungchan Cho [1,*] and Ilguk Jo [3,*]

[1] Department of Functional Composites, Korea Institute of Materials Science (KIMS), Changwon 51508, Korea; p996305s@kims.re.kr (S.S.); hyeonjae@kims.re.kr (H.P.); b.park@kims.re.kr (B.P.); leesb@kims.re.kr (S.-B.L.); lsk@kims.re.kr (S.-K.L.)

[2] School of Materials Science and Engineering, Pusan National University, Busan 46241, Korea; yangdo@pusan.ac.kr

[3] Department of Advanced Materials Engineering, Dong-Eui University, Busan 47340, Korea

* Correspondence: sccho@kims.re.kr (S.C.); ijo@deu.ac.kr (I.J.)

check for updates

Citation: Shin, S.; Park, H.; Park, B.; Lee, S.-B.; Lee, S.-K.; Kim, Y.; Cho, S.; Jo, I. Dispersion Mechanism and Mechanical Properties of SiC Reinforcement in Aluminum Matrix Composite through Stir- and Die-Casting Processes. *Appl. Sci.* **2021**, *11*, 952. https://doi.org/10.3390/app11030952

Academic Editor: Theodore E. Matikas

Received: 7 January 2021

Accepted: 19 January 2021

Published: 21 January 2021

Abstract: In this study, different volume fractions of silicon-carbide-reinforced AA2024 matrix composites were successfully fabricated using stir-casting (SC) and die-casting (DC) processes. The microstructural difference and physical properties of the composites during the manufacturing process were investigated in detail. The microstructural analysis found that the composite produced by the SC process had some reinforcement clusters and pores; however, defects and clusters significantly decreased after the DC process. In particular, the degree of reinforcement dispersion was quantitatively analyzed and compared before and after the DC process using the dispersion-analysis method. As a result of quantitative evaluation, the degree of dispersion was improved 2.5, 4.6, and 4.0 times with 3 vol.%, 6 vol.%, and 9 vol.% SiC-reinforced composite after the DC process, respectively. The electron backscatter diffraction (EBSD) analysis showed that the grain size of the 9 vol.% SiC-reinforced DC composite (17.67 µm) was 75% smaller than that of the SC composite (68.06 µm). The average tensile strength and hardness of the 9 vol.% SiC-reinforced DC composite were 2 times higher than those of the AA2024 matrix. The superior mechanical properties of the DC-processed composite can be attributed to the increase in dispersivity of the SiC particles and to decreases in defects and grain size during the DC process.

Keywords: Al matrix composites (AMCs); stir-casting (SC); die-casting (DC); dispersion mechanism; mechanical properties

1. Introduction

In recent decades, because of their properties of high strength-to-weight ratio and corrosion resistance, aluminum alloys have attracted attention as promising materials in many industries [1–3]. However, these alloys have application limits due to their absolute mechanical properties, which are lower than those of other structural materials (steel, titanium, etc.). To overcome this drawback, many studies have been performed to fabricate aluminum matrix composites (AMCs) with advanced mechanical properties by adding hard ceramic particulates such as SiC, B_4C, Al_2O_3, and TiB_2 [4–7]. Among many ceramic reinforcements, SiC has a similar density (3.21 g/cm^3) to that of Al (2.81 g/cm^3) and has excellent thermal and mechanical properties; thus, SiC is widely used as a reinforcement of metal matrix composites.

The manufacturing processes of AMCs can be classified into liquid, semi-solid, and solid-state processes [8]. The powder metallurgy process, which is a solid-state method, has the advantage of fabricating high-volume fraction composites; however, its drawbacks include a complex process and high cost [9]. On the other hand, liquid-state processes are known to be inexpensive and easy, with excellent productivity. However, liquid metal processes such as stir-casting (SC) make it difficult to ensure the uniform dispersion of ceramic particles in the matrix due to poor wettability and density differences [10–15]. Aykut Canakci et al. [16] investigated the mechanical properties of composites fabricated by SC. They found that fractures occurred at reinforcement agglomeration areas. They also found that it was very difficult to control the various defects (pores, clusters) during the SC process because there are many variables such as the shape and size of the particles, the design and position of the stirrer, the stirring speed, the operation and holding time, the mold temperature, the solidification speed, etc. [17–19]. Hence, to improve the quality of composites, it is necessary to conduct a subsequent process such as rolling, extrusion, or die-casting.

Die-casting (DC), a widely used metal-forming process, has many advantages compared to other methods, such as dimensional accuracy, near net shape, and high productivity. However, because of the difficulty of the process, few studies have been conducted on the microstructure and mechanical properties of Al matrix composites produced by DC. There have been attempts to fabricate AMCs using DC processes with control of the process parameters. Malomo et al. [20] fabricated bulk Al_2O_3/SiC/Al6061 composite by DC; they focused on the effects of optimum process parameters such as casting pressure, die design, and thickness on the composite properties. Hu et al. [21] investigated the effect of fluid shear, vacuum, and intensification pressure for particle distribution and pores formation. High pressure caused an increase in fluid velocity, which generated fluid shear force during mold filling. This may have contributed to the uniform particle distribution and reduction of the size of the pores. Dong et al. [22] fabricated high-performance TiB_2-reinforced Al-alloy composites via a super-vacuum-assisted die-casting process. The average grain size of α-Al in the matrix decreased by about 60% after the addition of TiB_2 nanoparticles; the grain refinement led to an improvement of the mechanical properties. The important factors in the DC composite process are the porosity, solidification rate, and, especially, dispersibility. However, there has been little research into the details of the dispersion mechanism or quantitative analyses of particles and their effects on the microstructure and mechanical properties of AMCs.

In this study, AA2024 matrix composites with 0, 3, 6, and 9 vol.% SiC were fabricated using both SC and DC processes. The microstructure and mechanical properties of the composites obtained by SC and DC processes were examined. The degree of particle dispersion was quantitatively analyzed by comparing differences between current and ideal distributions of reinforcement. Finally, effects of grain refinement during the solidification process of composites on the composite microstructure were schematically studied.

2. Materials and Methods

2.1. Materials and Casting Process

SiC-reinforced aluminum composites were fabricated by stir-casting (SC) and die-casting (DC). AA2024 alloy (DONG-YANG AK) was selected as the matrix material; its composition is listed in Table 1. As reinforcement, angular shaped SiC particles were used (30 µm, SAINT-GOBAIN).

Table 1. Composition of AA2024 alloy.

Elements	Si	Fe	Cu	Mn	Mg	Cr	Zn	Ti	Al
Weight %	0.05	0.08	4.00	0.46	1.32	0.06	0.02	0.02	Bal.

During the SC process, AA2024 alloy was completely melted by induction heating in a graphite mold at 700 °C and stirred at 900 rpm for 10 min. SiC particles were preheated in an electric furnace at 900 °C for two hours and then poured into the molten metal. The slag was removed, and molten metal was poured into a steel mold for air cooling after stirring.

Using a melting injection machine (KDM-400D, KOREA DIE CASTING MACHINERY, Incheon, Republic of Korea), the DC process was performed as post process. As-cast bulk composite using the SC process was die-cast into the mold, with conditions of 300 g casting weight and 250 °C mold temperature. The stir-cast composites were heated to 750–760 °C and held for 30 min; they were then injected into die molds, with 61 MPa pressure and injection speed with two steps of low (0.25 m/s) and high speed (4 m/s) to prevent mixing of external air [23].

2.2. Characterization

2.2.1. Microstructure Observation

The specimens were ground and polished down to 0.25 μm to obtain a clean surface. An optical microscope (LV100ND, NIKON, Tokyo, Japan) and a scanning electron microscope with energy-dispersive X-ray spectrometer (JSM-6610LV, JEOL, Tokyo, Japan) were used to observe the microstructure and reinforcement dispersion. In addition, a field-emission electron probe microanalyzer mapping device (JXA-8530F, JEOL, Tokyo, Japan) was used to confirm more details of the microstructure and precipitation in the matrix. An electron backscatter diffraction (JSM-7001F, JEOL, Tokyo, Japan) device was used to measure changes in the grain size.

2.2.2. Physical and Mechanical Property Measurement

The average density of the aluminum matrix composites (AMCs) was investigated by Archimedes principle from 5 measurements. The measured (actual) density and the theoretical density were calculated to confirm the porosity of the specimens. The theoretical density was calculated using rule of mixtures, as in the equation below.

$$\rho_{theoretical} = \rho_{matrix} * V_{matrix} + \rho_{reinforcement} * V_{reinforcement}$$

where ρ is the density of the matrix and reinforcement and V is the volume fraction of each material.

A tensile test was performed using a universal testing machine (5882 model, INSTRON, Norwood, MA, USA) with 5×10^{-3} s^{-1} head speed. Subsize dog-bone-shape specimens were prepared (1.5 mm thickness, 2 mm width, and 5 mm gage length). A hardness test was performed using a Rockwell hardness tester (HR-210MR, MITUTOYO, Kawasaki, Japan) following the ASTM E18 standard. The average hardness values were calculated after measuring specimens 5 times each. An indenter was used with 1/16 (Φ 1.588 mm) steel balls at B scale.

2.2.3. Dispersion Evaluation

Distances between individual SiC reinforcements in the AMCs were calculated from microscopic images to quantitatively evaluate reinforcement dispersion in the composite. Then, the distance distribution of the composite was compared with that of an ideal composite with perfectly dispersed reinforcements. The difference between the current and the ideal distributions was presented as a single index called the dispersion index (DI). By comparing the DIs of various AMCs with different processing conditions, it was determined how each parameter affected the reinforcement dispersion in the final composite products. The aforementioned evaluation process was performed using in-house software developed by the author group [24].

3. Results and Discussion

3.1. Microstructure and Reinforcement Dispersion

The microstructures of the AA2024 alloy and SiC/AA2024 composite are shown in Figure 1a–h. SEM and EDS analyses revealed that black-colored SiC particles were distributed in the Al matrix. In the case of AA2024 (Figure 1a), after the stir-casting (SC) process, small pores (marked as blue-dot circles) were observed throughout the matrix. With the reinforcement-particle addition, relatively large micropores could be observed. These are marked with yellow arrows in Figure 1b–d. Porosity increases with particle addition are attributed to the generation of particle agglomeration and clustering during solidification [25,26]. The microstructures of the matrix and of the AMCs that were fabricated by the die-casting (DC) process are shown in Figure 1e–h. In Figure 1d, pores and cracks are not observed in the matrix alloy. In addition, it was confirmed that the dispersion of the SiC reinforcement was uniform, and micropores were almost completely removed near the agglomerated particles (Figure 1f–h). Microstructural images also show that the grain size of the AMCs is smaller than that of the base alloy because the added reinforcements act as heterogeneous nucleation sites during solidification [27]. Moreover, for the same volume fraction, the grain size of AMCs produced by the DC process was much smaller than that of AMCs fabricated by SC because of the different cooling rates of the two processes.

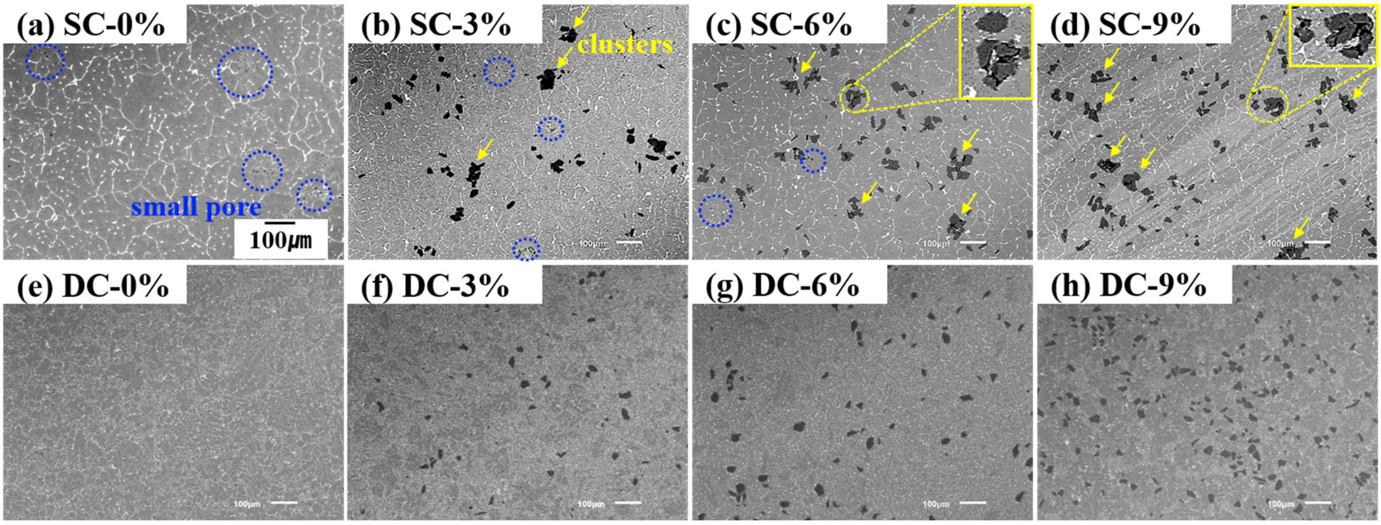

Figure 1. Microstructure of AA2024 alloy and aluminum matrix composites (AMCs) formed by the stir-casting (SC) process: (**a**) AA2024, (**b**) 3 vol.%, (**c**) 6 vol.%, (**d**) 9 vol.%, and after the die-casting (DC) process, (**e**) AA2024, (**f**) 3 vol.%, (**g**) 6 vol.%, (**h**) 9 vol.% (same magnification).

To better understand the composition of the grain boundary precipitates, field-emission electron probe microanalyzer (FE-EPMA) microstructure-mapping observation was conducted on the 9 vol.% SiC/AA2024 composite before (Figure 2a) and after the DC process (Figure 2b). In all microstructural images, a thin white band is observed, similar to that in the scanning electron microscope (SEM) images of the matrix; this band confirms the presence of Al-Cu and Al-Cu-Mg intermetallic compounds and precipitation trapped in the grain boundary. As can be seen from the EPMA analysis, after the DC process, the specimen had more uniform particle dispersion without agglomeration than that of the SC composite. As the size of the grains decreased due to the DC process, the size of the intermetallic phases decreased, and the dispersion increased.

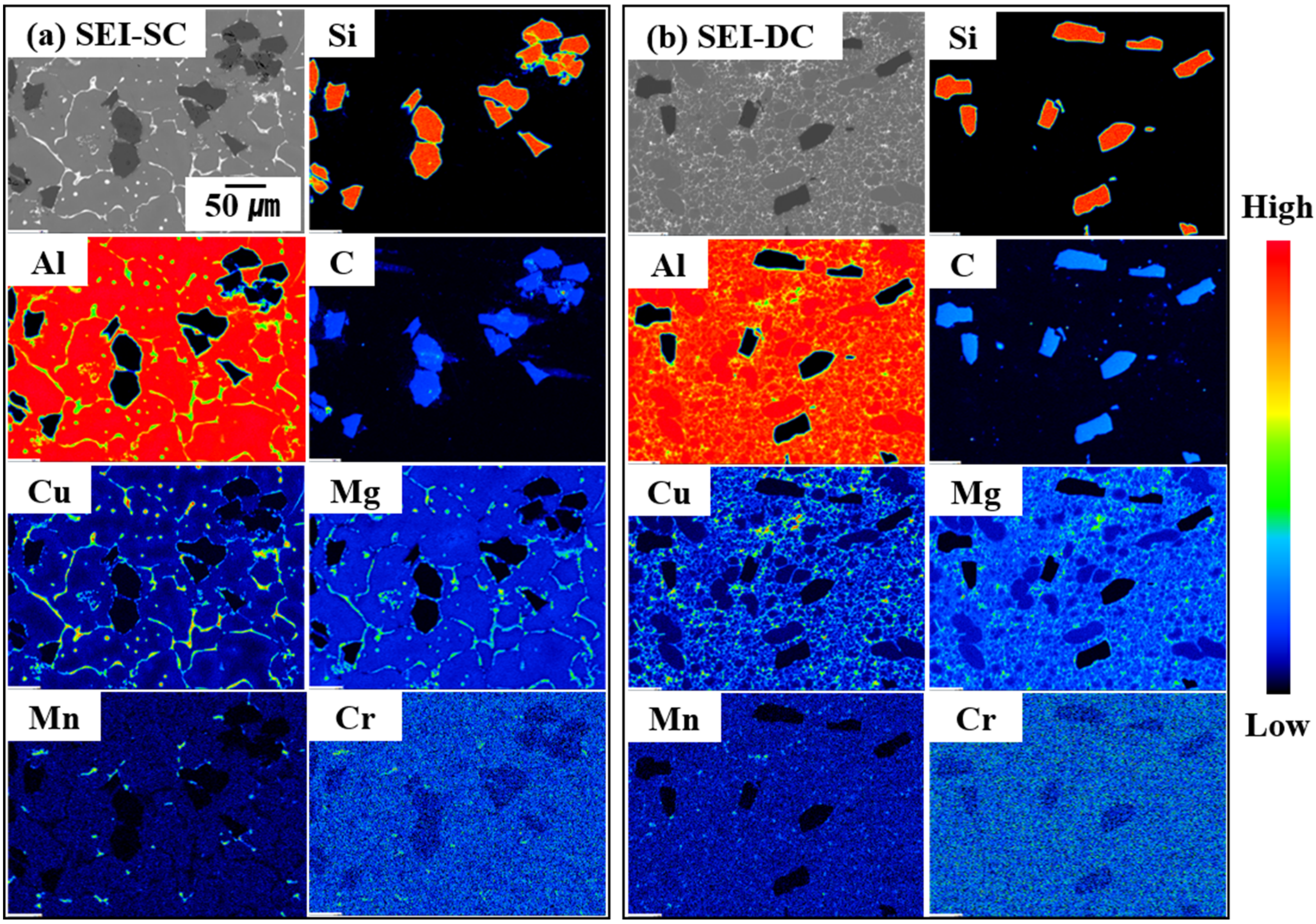

Figure 2. Results of electron probe microanalyzer (EPMA) elemental mapping at 9 vol.% SiC/AA2024: (**a**) SC process, (**b**) DC process.

To evaluate the pore amounts in the AA2024 alloy and the composite after SC and DC processes, the actual and theoretical density were measured, and the results are shown in Table 2. The porosity was confirmed to be 3.8%, 4%, 5%, and 5.4% for the 0, 3, 6, and 9 vol.% SiC-reinforced stir-cast specimens, respectively. Previous studies already showed the approximate quadratic polynomial equation correlation between the volume fraction of the reinforcement and the porosity; the equation is as follows:

$$P = 2.19 + 0.36 \times (S) - 0.006 \times (S)$$

where P is the percent of porosity and S is the volume fraction of particles in the casting. The calculation implies that the porosity continues to increase to a 30 volume percent of reinforcement and then decreases after this critical point. Therefore, the relative density slightly decreased (porosity increased) as the volume fraction increased in these volume fraction ranges. These effects are thought to result from the amount of air sucked inside the liquid metal vortex during the stir process. In addition, the generation of particle clusters is more active at low volume fraction than at high volume fraction. In the case of high volume fraction, there is a relatively low fluidity of the melt, and the large number of particles tend to physically restrict their own movement. Thus, the generation and growth of clusters are suppressed, and there are fewer clusters. On the other hand, the physical suppression of cluster generation is different between cases of high volume fraction and low volume fraction, and high fluidity of the melt can make particles move easily. For this reason, moving particles gathered into specific areas and formed clusters [28].

Table 2. Density of AA2024 and aluminium matrix composites (AMCs) in stir-casting (SC) and die-casting (DC) processes.

Density	Stir-Casting				Die-Casting			
	AA2024	3 vol.%	6 vol.%	9 vol.%	AA2024	3 vol.%	6 vol.%	9 vol.%
Actual density (g/cm^3)	2.674	2.680	2.665	2.666	2.757	2.788	2.782	2.786
Theoretical density (g/cm^3)	2.780	2.793	2.806	2.818	2.780	2.793	2.806	2.818
Relative density (%)	96.2	96.0	95.0	94.6	99.2	99.8	99.1	98.9

Reinforcement was uniformly distributed after the DC process, and micropores are not found in the microstructure images. The porosity considerably decreased compared to that of AMCs produced by SC process. The porosity values of the DC composites were confirmed to be 0.8%, 0.2%, 0.9%, and 1.1%. The dispersion of particles improved and the porosity decreased after the DC process, largely because of the two factors of fast cooling rate and fluid shear force. Conventional high-pressure die-casting (HPDC) has attractive advantages in that the process can induce fluid shear and high cooling rate. Aggregated particles are dispersed by the fluid shear force at high pressure, and the movement time of reinforced particles is minimized by the fast cooling rate. In addition, grains are critically refined with the increase of nucleation sites and rapid solidification. Thus, pores generated by agglomerated particles decrease because of the elimination of clusters and the rearrangement of particles.

More details of both mechanisms of solidification are shown in Figure 3. Considering the schematic diagram, particles that are well-dispersed by fluid shear force can create many heterogeneous nucleation sites in the early stage of solidification, and primary α-Al phases are generated and grown. In middle of the solidification, the fast cooling rate of the DC process can lead to grain refinement. A number of liquid–solid surfaces are gradually enlarged by refined primary α-Al dendrite, and this can push particles to the last solidification zone (grain boundary). Therefore, coarse grains with a slow cooling rate push particles in a small specific area, and this causes agglomeration of the particles; however, fine grains with fast solidification speed push the particles in various directions to large areas (grain boundary or last freezing zone) [29–31].

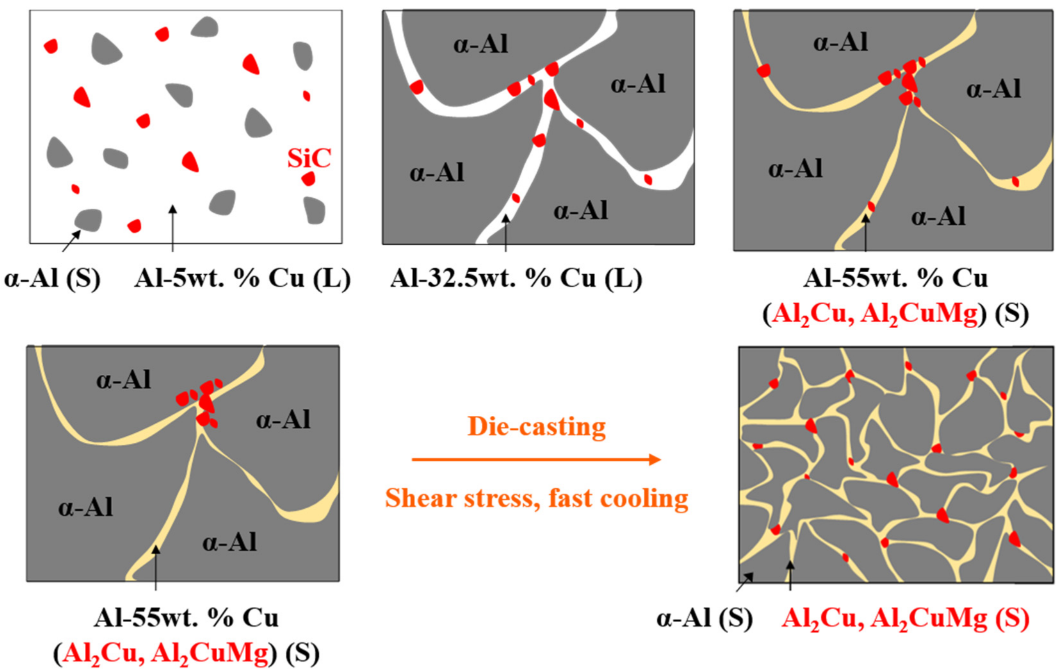

Figure 3. Schematic diagram of solidification behavior of SiC/AA2024 AMCs.

The grain size was observed by electron backscatter diffraction (EBSD) analysis (Figure 4) to determine the average grain size of SC- and DC-processed 9 vol.% SiC-reinforced specimens. In Figure 4, the black color indicates SiC particles; the average grain sizes are 68.06 µm (SC, Figure 4a) and 17.67 µm (DC, Figure 4b), respectively. It is confirmed that the average grain size decreases by about 75% due to grain refinement from the fast cooling rate of the DC process. The addition of SiC particles and the fast cooling rate during the DC process increase the grain-refinement effect of the SiC/AA2024 composite, which might contribute to strengthening of the composite.

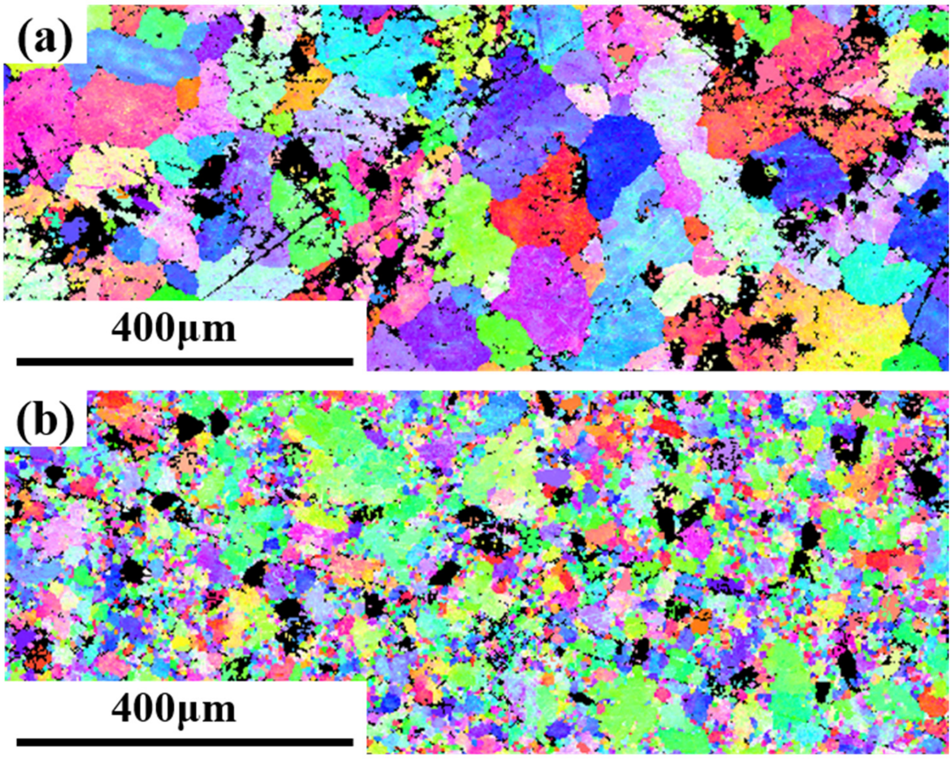

Figure 4. Results of the electron backscatter diffraction (EBSD) analysis of 9 vol.% SiC/AA2024: (**a**) stir-casting (SC) process, (**b**) die-casting (DC) process.

As mentioned, we believe that the DC process improves SiC dispersion in SiC/AA2024 AMCs, and this improvement is qualitatively presented with microscopic images and EBSD-analysis results. To quantitatively evaluate the effect of DC in reinforcement-dispersion improvement, an automated image-processing program with a statistical approach was applied. First, the program automatically studied the characteristics of reinforcement-particle images. Then, based on the learned reinforcement characteristics, the program extracted only reinforcement particles from the given microscopic image. Finally, the dispersion of extracted reinforcements was analyzed. The nearest neighbor (NN) distances between each reinforcement followed a Weibull distribution with a scale parameter λ and shape parameter k. This is an N-body problem in macroscopic volume. λ corresponds to the Wigner–Seitz radius [32] or the reinforcement content of the composite; k indicates the dimensions of the image (2D or 3D). The NN distances were calculated from the processed image, and distributions $W_a(\lambda_a, k_a)$ were compared with the ideal distribution $W_i(\lambda_i, k_i)$. Finally, the dispersion index (DI) was defined as the distribution parameter difference between W_a and W_i, as follows (a smaller DI implies better reinforcement dispersion):

$$0 \le \mathrm{DI} = \sqrt{\left|\left(1 - \frac{\lambda_\mathrm{a}}{\lambda_e}\right)\left(1 - \frac{k_\mathrm{i}}{k_\mathrm{i}}\right)\right|} \le 1$$

Figures 5 and 6 present calculated DI values of AMCs after SC and DC processes. In each case, a grayscale microscopic image of an AMC sample has been processed into a blue matrix and yellow reinforcements. The calculated NN distances between each reinforcement are presented as a histogram and fitted as a Weibull distribution (blue dashed line). This distribution is compared with the ideal distribution (red solid line) to evaluate the DI. The DI was decreased at the same volume fraction after the DC process, from 0.2564 to 0.1085 at 3 vol%, 0.2303 to 0.0537 at 6 vol%, and 0.1671 to 0.0464 at 9 vol% SiC content. A decreased DI implies that the distribution parameter of the actual NN-distance distribution is closer to the ideal distribution, corresponding to a homogeneous reinforcement dispersion. Thus, decreased DI values in the die-cast samples indicate the effectiveness of the DC process in improving the reinforcement dispersion. Furthermore, these results match well with qualitative dispersion enhancements observed in the original microscopic images and EBSD analyses.

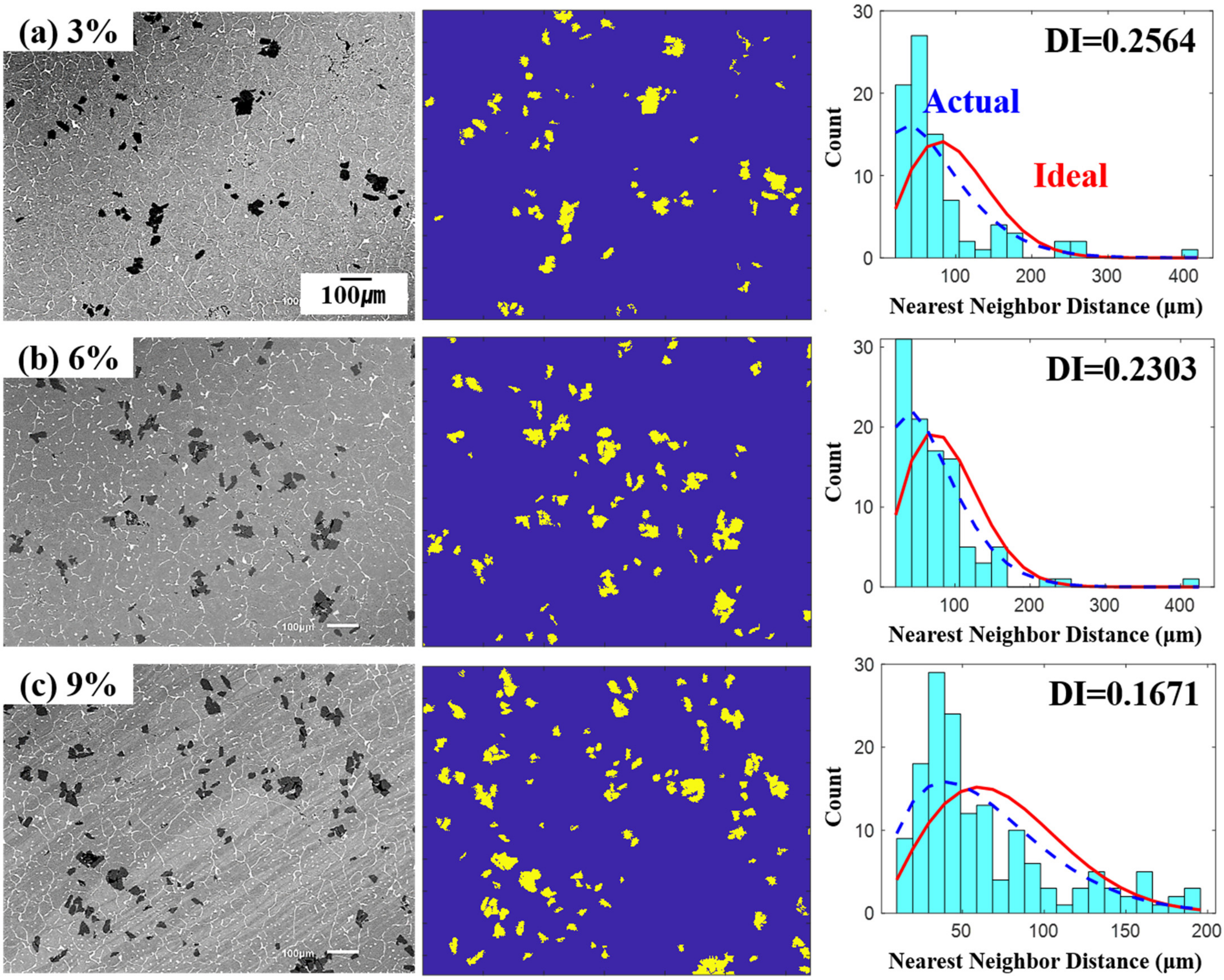

Figure 5. Degree of particle dispersion by the SC process: (**a**) 3 vol.%, (**b**) 6 vol.%, and (**c**) 9 vol.%.

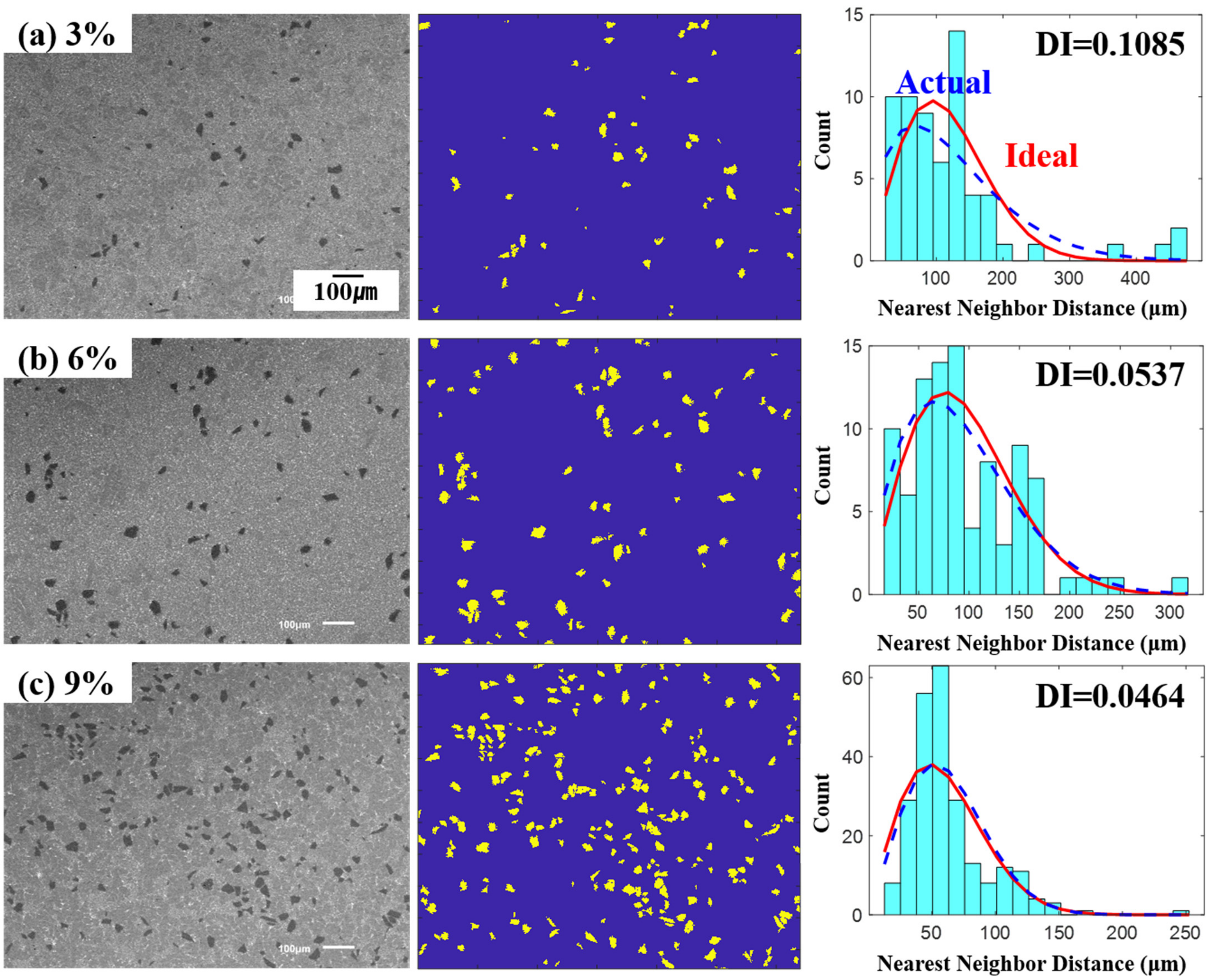

Figure 6. Degree of particle dispersion by the DC process: (**a**) 3 vol.%, (**b**) 6 vol.%, and (**c**) 9 vol.%.

3.2. Mechanical Properties

The results of the Rockwell hardness test of the AMCs are shown in Figure 7. The standard deviation of the hardness value tended to decrease gradually, and the absolute hardness value increased as the volume fraction of SiC increased in both processes. Generally, for the same particle size, the hardness increases as the volume fraction of the reinforcement increases [33,34]. In addition, the standard deviation of the hardness decreases as the degree of dispersion improves (i.e., smaller DI value). The deviation of the hardness value in the product of the SC process was larger than in the DC process; this is because of the presence of particle agglomeration and pores. This means that the deviation of the same sample depends on where the indenter is put to make measurements, such as in the agglomeration particle region or in an area with a lack of particles. However, the hardness results show that deviation of the hardness values rarely occurs in samples subject to the DC process, which means that the dispersion of particles was improved. The maximum hardness value was 57.6 HRB at 9 vol.%; this is about 30% higher than the hardness value of the matrix and 32% higher than that of AMCs fabricated by the SC process with the same volume fraction of particles.

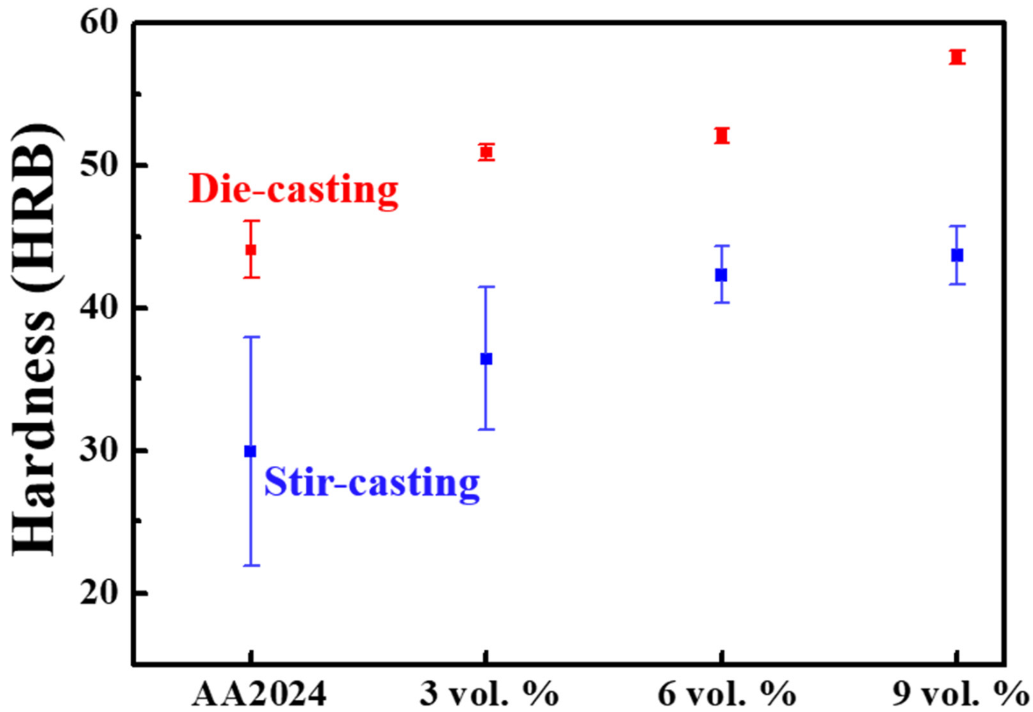

Figure 7. Results of Rockwell hardness (B scale) measurement.

Tensile stress–strain curves of the AMCs are shown in Figure 8. The blue line shows the results of the SC AMCs, while the red line shows the results of AMCs fabricated by the DC process. In the stir-cast specimens, tensile strength and elongation decreased slightly as the volume fraction of SiC increased because particle agglomeration and pores caused stress concentration and so the mechanical properties of the AMCs decrease [35,36]. On the other hand, there tended to be increases in tensile strength and elongation in the die-cast specimens. The ultimate tensile strength value was 313.7 MPa, which is two times higher than the SC results, and the elongation was four times greater than was seen in the SC results. As confirmed in previous dispersion results, aggregated particles and pores were removed via the DC process, and the dispersion became uniform. Changes in the microstructure led to improvement of interfaces between particles and matrix. Thus, tensile strength and elongation improved because load transfer from the matrix to the reinforcement was efficiently preformed [37]. In addition, we believe that there was slight strengthening as a result of grain refinement, as in the previous results of Amirkhanlou et al. [38].

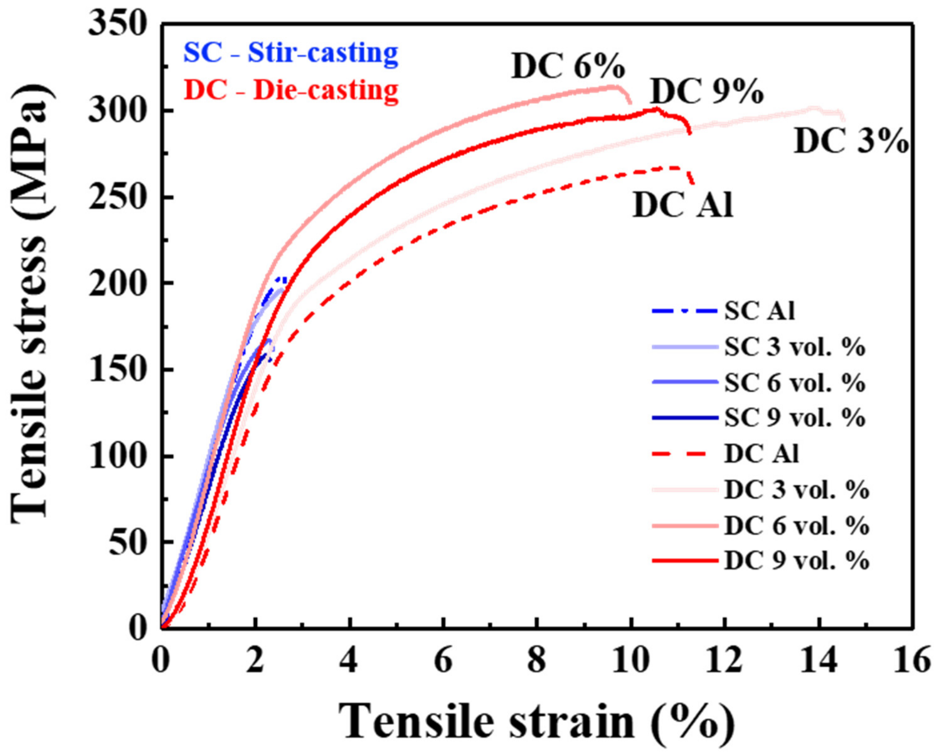

Figure 8. The stress–strain curves of the AMCs with different process.

4. Conclusions

This study fabricated a sound SiC/AA2024 metal matrix composite using stir-casting (SC) and die-casting (DC) processes. Effects of the DC process were confirmed to allow comparison of the effects of the two process types on the Al composites, and the microstructures and mechanical properties of specimens of various volume fractions were evaluated.

1. Microstructural observation showed particle clusters and pores in the aluminum matrix composites (AMCs) after the SC process. After the DC process, agglomerations and pores were removed and the particle distribution was more uniform than in the case of AMCs formed by the SC process. This is attributed to two-stage melt injection during the DC process prevented air inflow and induced rapid solidification, which led to grain refinement and uniform particle dispersion.
2. The grain size of the DC-processed composite was 17.67 μm, which is approximately a 75% decrease compared to the composite fabricated by the SC process (68.06 μm). This result shows that the grain refinement might contribute to strengthening the composite. Moreover, with the DC process, the degree of dispersion of SiC particles increased. The distribution of the reinforcement was quantitatively analyzed, and the results showed decreased dispersion index (DI) values for die-cast samples, which indicates the effectiveness of the DC process in improving the reinforcement dispersion.
3. The deviation of the hardness value decreased after the DC process. Especially, the maximum hardness value was 57.6 HRB at 9 vol.% SiC; this is an approximately 30% higher value than that of the matrix. Moreover, the hardness of the DC composite improved by about 32% compared to that of the AMCs fabricated by the SC process at the same volume fraction.
4. In the case of specimens fabricated by the SC process, the tensile strength decreased as the volume fraction of SiC particles increased. On the other hand, specimens manufactured by the DC process tended to show increased tensile strength and elongation as the volume fraction increased. The maximum tensile strength was 313.7 MPa for the DC process, which is about two times higher than that of the composite produced by the SC process; the elongation increased by about four times.

These results are attributed to the uniformly dispersed particles, which caused the load to transfer efficiently from matrix to reinforcement as well as to the strengthening effect of grain refinement in the DC process.

Author Contributions: Conceptualization, S.-K.L. and I.J.; methodology, S.C.; software, B.P.; validation, S.-B.L.; formal analysis, H.P.; investigation, S.S.; data curation, Y.K.; writing—original draft preparation, S.S.; writing—review and editing, I.J.; visualization, B.P.; supervision, I.J.; project administration, S.C.; funding acquisition, S.C. All authors have read and agreed to the published version of the manuscript.

Funding: This research was financially supported by the Fundamental Research Program (PNK7380) of the Korea Institute of Materials Science.

Institutional Review Board Statement: Not applicable.

Informed Consent Statement: Not applicable.

Data Availability Statement: The data and analysis in this study are available on request from the corresponding author.

Acknowledgments: This research was supported by the Basic Science Research Capacity Enhancement Project through a Korea Basic Science Institute (Core-facility for Converging Materials) grant funded by the Ministry of Education (2019R1A6C1010045).

Conflicts of Interest: The authors declare no conflict of interest.

References

1. Shorowordia, K.M.; Laouib, T.; Haseeba, A.S.M.A.; Celisb, J.P.; Froyenb, L. Microstructure and interface characteristics of B_4C, SiC and Al_2O_3 reinforced Al matrix composites: A comparative study. *J. Mater. Process. Technol.* **2003**, *142*, 738–743. [CrossRef]
2. Dwivedi, S.P. Microstructure and mechanical behavior of Al/B_4C metal matrix composite. *Mater. Today. Proceedings.* **2020**, *25*, 751–754. [CrossRef]
3. Suresh, S.; Moorthi, N.S.V. Process development in stir casting and investigation on microstructures and wear behavior of TiB_2 on Al6061 MMC. *Procedia Eng.* **2013**, *64*, 1183–1190. [CrossRef]
4. Mohapatra, J.; Nayak, S.; Mahapatra, M.M. Mechanical and tribology properties of Al-4.5%Cu-5%TiC metal matrix composites for light-weight structures. *Inter. J. Lightweight Mater. Manufac.* **2020**, *3*, 120–126. [CrossRef]
5. Sajjadi, S.A.; Ezatpour, H.R.; Beygi, H. Microstruxture and mechanical properties of Al-Al_2O_3 micro and nano composites fabricated by stir casting. *Mater. Sci. Eng. A.* **2011**, *528*, 8765–8771. [CrossRef]
6. Maurya, N.K.; Maurya, M.; Srivastava, A.K.; Dwivedi, S.P.; Kumar, A.; Chauhan, S. Investigation of mechanical properties of Al6061/SiC composite prepared through stir casting technique. *Mater. Today. Proceedings.* **2020**, *25*, 755–758. [CrossRef]
7. Iwaszko, J.; Kudla, K. Effect of friction stir process (FSP) on microstructure and hardness of AlMg10/SiC composite. *Bull. Pol. Ac. Sci.* **2019**, *67*, 185–192.
8. Srivatsan, T.S.; Ibrahim, I.A.; Mohamed, F.A.; Lavernia, E.J. Processing techniques for particulate-reinforced metal aluminium matrix composites. *J. Mater. Sci.* **1991**, *26*, 5965–5978. [CrossRef]
9. Arif, S.; Alam, M.T.; Ansari, A.H.; Siddiqui, M.A.; Mohsin, M. Investigation of Mechanical and Morphology of Al-SiC composites processed by PM Route. *Mater. Sci. Eng.* **2017**, *255*, 012277. [CrossRef]
10. Hashim, J.; Looney, L.; Hashmi, M.S.J. Metal matrix composites: Production by the stir casting method. *J. Mater. Process. Technol.* **1999**, *92-93*, 1–7. [CrossRef]
11. Prasad, V.J.; Rao, N.M.; Kamaluddin, S. A Study of Microstructure and Tribological Properties of Stir Cast Al Metal Matrix Composite. *Mater. Today Proc.* **2017**, *4*, 9264–9271. [CrossRef]
12. Kumar, R.A.; Krishnakumar, T.S. Casting and characterization of Al6063/SiC nano composites produced using stir casting method. *Mater. Today Proc.* **2018**, *5*, 23853–23862. [CrossRef]
13. Kaushika, N.; Singhal, S. Dry-Sliding Wear Analysis of SiC Reinforced AA6063 As-Cast Aluminum Metal Matrix Composites. *Mater. Today Proc.* **2018**, *5*, 24147–24156. [CrossRef]
14. Vanam, J.P.; Chiranjeevi, R.; Kumar, R.S.; Ramana, V.S.N.V.; Kumar, A.S. Effect of SiC on Mechanical, Microstructure and Tribological properties of Aluminum MMC processed by Stir Casting. *Mater. Sci. Eng.* **2018**, *455*, 012017. [CrossRef]
15. Saenpong, P.; Talangkun, S.; Laonapakul, T.; Boonma, A. Microstructures and hardness of A356-SiC composites produced by the mechanical stir casting. *Mater. Today Proc.* **2018**, *5*, 9489–9496. [CrossRef]
16. Canakci, A.; Arslan, F.; Varol, T. Physical and mechanical properties of stir-casting processed AA2024/B_4C_p composites. *Sci. Eng. Mater.* **2014**, *21*, 505–515. [CrossRef]
17. Ambhai, K.G. Study on machinability of Al-SiC particulate metal matrix composite. Ph.D. Thesis, Metalergical Engineering Department, Indian Institute of Technology, Roorkee, India, 2007.

18. Sato, A.; Mehrabian, R. Aluminium matrix composites: Fabrication and properties. *Metall. Trans. B.* **1976**, *7*, 443–451. [CrossRef]
19. Naher, S.; Brabazon, D.; Looney, L. Simulation of the stir casting process. *J. Mater. Process. Technol.* **2004**, *143–144*, 567–571. [CrossRef]
20. Malomo, B.O.; Ogunbodede, O.T.; Popoola, O.T.; Oluwasegun, K.M.; Ibitoye, S.A.; Adekoya, L.O. A Design Optimization of the High Pressure Die Casting Process for the Fabrication of Bulk Metal Matrix Composites. *Mater. Perfom. Charact.* **2017**, *6*, 535–550. [CrossRef]
21. Hu, Q.Y.; Zhao, H.D.; Li, F.D. Microstructures and properties of SiC particles reinforced aluminum matrix composites fabricated by vacuum-assisted high pressure die casting. *Mater. Sci. Eng. A.* **2017**, *680*, 270–277. [CrossRef]
22. Dong, X.; Youssef, H.; Zhnang, Y.; Wang, S.; Ji, S. High performance Al/TiB_2 composites fabricated by nanoparticle reinforcement and cutting-edge super vacuum assisted die casting process. *Composites Part B.* **2019**, *177*, 107453. [CrossRef]
23. Itamura, M.; Yamamoto, N. Effects of Dual Speed Injection on Quality and Metal Flow of plate Shape Die Casting. *J. Japan Foundry Eng. Soc.* **1996**, *68*, 242–248.
24. Park, B.; Lee, D.; Jo, I.; Lee, S.B.; Lee, S.K.; Cho, S. Automated quantification of reinforcement dispersion in B_4C/Al metal matrix composites. *Composites Part B.* **2020**, *181*, 107584. [CrossRef]
25. Sajjadi, S.A.; Ezatpour, H.R.; Parizi, M.T. Comparison of microstructure and mechanical properties of A356 aluminum alloy/Al_2O_3 composites fabricated by stir and compo-casting processes. *Mater. Des.* **2012**, *34*, 106–111. [CrossRef]
26. Kok, M. Production and mechanical properties of Al_2O_3 particle-reinforced 2024 aluminium alloy composites. *J. Mater. Proc. Technol.* **2005**, *161*, 381–387. [CrossRef]
27. Bharath, V.; Nagaral, M.; Auradi, V.; Kori, S.A. Preparation of 6061Al-Al_2O_3 MMC's by Stir Casting and Evaluation of Mechanical and Wear Properties. *Procedia Mater. Sci.* **2014**, *6*, 1658–1667.
28. Bindumadhavan, P.N.; Chia, T.K.; Chandrasekaran, M.; Wah, H.K.; Lam, L.N.; Prabhakar, O. Effect of particle-porosity clusters on tribological behavior of cast aluminum alloy A356-SiC_p metal matrix composites. *Mater. Sci. Eng. A.* **2001**, *315*, 217–226. [CrossRef]
29. Ravi, K.R.; Pillai, R.M.; Amaranathan, K.R.; Pai, B.C.; Chakraborty, M. Fluidity of aluminum alloys and composites: A review. *J. Alloy Compd.* **2008**, *456*, 201–210. [CrossRef]
30. Zhang, Z.; Chen, X.G.; Charette, A. Particle distribution and interfacial reactions of Al–7% Si–10% B_4C die casting composite. *J. Mater. Sci.* **2007**, *42*, 7354–7362. [CrossRef]
31. Costanza, G.; Quadrini, F.; Tata, M.E. Pressure effect on Al alloys cast behavior: Microstructures and mechanical properties. J. *Mater. Prod. Technol.* **2004**, *20*, 345–357. [CrossRef]
32. Girifalco, L.A. *Statistical Mechanics of Solids*; Oxford University Press: New York, NY, USA, 2003.
33. Cerit, A.A.; Karamis, M.B.; Nair, F.; Yildizli, K. Effect of Reinforcement Particle Size and Volume Fraction on Wear Behaviour of Metal Matrix Composites. *Tribo. Ind.* **2008**, *14*, 482–489.
34. Canakci, A.; Varol, T.; Ozsahin, S. Prediction of Effect of Volume Fraction, Compact Pressure and Milling Time on Properties of Al-Al_2O_3 MMCs Using Neural Networks. *Met. Mater. Int.* **2013**, *19*, 519–526. [CrossRef]
35. Segurado, J.; Lez, C.G.; Llorca, J. A numerical investigation of the effect of particle clustering on the mechanical properties of composites. *Acta Materialia.* **2002**, *51*, 2355–2369. [CrossRef]
36. Deng, X.; Chawla, N. Modeling the effect of particle clustering on the mechanical behavior of SiC particle reinforced Al matrix composites. *J. Mater. Sci.* **2006**, *41*, 5731–5734. [CrossRef]
37. Bonneville, J.; Laplanche, G.; Joulain, A.; Brunet, V.G.; Dubois, S. Al-matrix composite materials reinforced by Al-Cu-Fe particles. *J. Phys. Conf. Ser.* **2010**, *240*, 012013. [CrossRef]
38. Amirkhanlou, S.; Rahimian, M.; Ketabchi, M.; Parvin, N.; Yaghinali, P.; Carreno, F. Strengthening Mechanisms in Nanostructured Al/SiC_p Composite Manufactured by Accumulative Press Bonding. *Metall. Mater. Trans. A.* **2016**, *47*, 5136–5145. [CrossRef]